VENUE ENVIRONMENT MONITORING AND INTELLIGENT REGULATION SYSTEM BASED ON IMPROVED RBF NEURAL NETWORK AND ZIGBEE TECHNOLOGY

Yi Pan, Yanjun Hu*
School of Mechanical and Electrical Engineering, Yueyang Vocational Technical College, Yueyang 414000, China

Abstract - In response to the problems of large venue environments with large spans and strong dynamic coupling, which make traditional control difficult to meet monitoring and control requirements, this study designs an environmental monitoring and intelligent regulation system based on Zigbee technology. This study designs a venue environment control system based on Zigbee technology and introduces an improved radial basis function neural network to correct the monitoring error of venue environment data. Finally, this study employs an improved deep reinforcement learning approach (Proximal Policy Optimization, PPO) to construct a venue environment regulation model. Specifically, by integrating the spatial attention mechanism, the control focuses on high-density crowd areas is enhanced, and the objective function is optimized through adaptive cropping coefficients, which dynamically balance exploration and utilization during the training process, achieving precise control of venue environmental parameters. In the venue environment monitoring experiment, the research model shows the best performance, achieving a monitoring accuracy of 98.25% in temperature monitoring. In the error testing of environmental humidity monitoring, the maximum relative error of the research model is 1.02%, which is superior to similar models. In temperature target regulation, the research model is closer to the target of 26 ℃ and has the smallest deviation. In multi-objective regulation, the accuracy and uniformity of the research model in light testing are 0.975 and 35.568 lx, with the best overall test results. The proposed technology has shown good application effects in venue environmental monitoring and regulation, providing technical support for high-precision and low-energy consumption environmental control of venues.

Keywords: Zigbee Mesh; Improved RBF; PPO; Venue environment; Regulation.

1. Introduction

Zigbee adopts the IEEE 802.15.4 low-power network protocol standard, which operates in the 2.4 GHz frequency band and features low cost, low power consumption, self-organization, and self-healing capabilities. It is widely used in the field of the Internet of Things (IoT) [1]. Due to its open protocol stack and license-free frequency band, Zigbee has a wide range of applications in smart homes, environmental monitoring, industry, agriculture, and other scenarios, making it the preferred communication technology for intelligent regulation systems [2]. In addition, with the development of information technology, sensor networks and various control algorithms are integrated, and through communication hubs, precise parameter control is achieved for greenhouses, streetlights, and home systems [3]. Jogekar et al. proposed an IoT-based real-time security system to address issues such as low efficiency and poor monitoring accuracy in underground mine gas monitoring. It used ZigBee technology as the wireless communication foundation, deployed location sensors to evaluate environmental variables and gas thresholds, and constructed an intelligent control system. ZigBee technology could achieve communication in tunnels over 100 m deep and achieve high-precision environmental monitoring [4]. Ruzibaeva et al. conducted research on the communication coverage problem in traditional English classrooms and developed an intelligent English learning system using an improved ZigBee algorithm and Wireless Sensor Network (WSN). This system could cover the entire teaching environment and optimize the teaching network. Tests have shown that all network nodes have good communication performance and effectively improve teaching quality [5]. Romputtal

dx.doi.org/10.17683/ijomam/issue24.3

et al. proposed a 2.4GHz T-slot antenna embedded ZigBee WSN system to address the limitations of data storage in traditional ZigBee systems. This study obtained antenna parameters through simulation, made gateway and sensor node boards, and tested them to construct an IoT monitoring scheme and conduct experiments. The system had good anti-interference ability and met the low latency requirements for long-distance communication [6].

In recent years, deep learning has been widely applied in the fields of data mining, prediction, and regulation, especially in environmental regulation with outstanding results. Relevant scholars have conducted extensive research on this. Manikandan R et al. conducted research on the problem of traditional agriculture relying on manual labor and low management efficiency, and proposed a sensor-based intelligent control system. The system combined IoT sensors such as humidity and temperature, used deep control algorithms to accurately measure environmental parameters, and achieved effective environmental control through a logic controller. The system had precise environmental regulation capabilities, which have increased the yield of agricultural crops [7]. Zhou Y et al. conducted research on the difficulty of achieving precise environmental monitoring with self-powered wireless sensors and designed an automatic control system driven by machine learning algorithms. It achieved precise temperature and humidity control in the environment through parameter optimization. The system had excellent environmental monitoring capabilities, significantly improving the accuracy of droplet equipment [8]. Guo D et al. conducted research on the problem of difficulty in ensuring uniform and stable humidity in centralized humidity control of buildings, and proposed an intelligent distributed humidity control system based on model-free deep reinforcement learning. The system consisted of intelligent controllers and incorporated deep reinforcement algorithms to reduce environmental monitoring errors. It could accurately monitor and regulate environmental humidity conditions, which is superior to similar systems [9]. Özen F et al. conducted research on the difficulty of accurately predicting temperature and humidity, and created a model system for specific regions that integrates meteorological bureau and multi-sensor data. In addition, the study used an LSTM algorithm for prediction and developed a management system in conjunction with an IoT framework. This system had excellent communication and temperature and humidity control capabilities, but its adaptability to abnormal climate data was weak [10].

According to the above research, with the development of IoT and deep learning technologies, Zigbee technology has been widely used in environmental monitoring, intelligent regulation, and other fields due to its low cost, low power consumption, and self-organizing ability, providing support for multi-scenario parameter acquisition and transmission [11]. However, in environmental monitoring, it mainly adopts control technologies such as constant temperature and humidity or fixed threshold, which can only control a single environmental variable and cannot meet the environmental control requirements in large venues [12]. To solve the problem of insufficient regulation of venue environment, this study proposes a venue environment monitoring and intelligent regulation system based on improved an Radial Basis Function Neural Network (RBF) and Zigbee technology to improve the quality of the venue environment. This study has two innovations. One is to adopt Zigbee Mesh+data aggregation low-power architecture and design a venue environment control system to meet the high-performance communication requirements of the venue. The second is to adopt improved RBF and deep reinforcement learning to construct an integrated architecture for venue environment monitoring and regulation, achieving high-precision regulation of the venue environment. This study can provide technical support for efficient and stable environmental monitoring and intelligent regulation of venues, and improve the quality of the venue environment.

2. Research Design

2.1 Design of Venue Environment Control System based on Zigbee Technology

As a densely-populated and open public area, the environmental parameters of large venues will directly affect human comfort and equipment operation efficiency. Traditional venues use wired monitoring systems, which cannot meet the dynamic control requirements of indoor environments and have high maintenance costs. This study proposes a venue environment control system based on Zigbee technology, as shown in Figure 1.

In Figure 1, the system is based on Zigbee technology for communication and adopts a three-layer architecture design of "perception layer, network layer, application layer". The perception layer consists of sensor nodes distributed in various areas of the venue, involving temperature and humidity sensors, CO2 sensors, and lighting sensors. To meet the data collection requirements of the nodes in the venue, CC2538 is used as the control chip for the node hardware. The temperature sensor adopts SHT30, with a monitoring range of -40 ℃~125 ℃ and an accuracy of ± 0.3 ℃/± 2% RH. The CO2 sensor is SCD41, which meets the monitoring range of 400 ppm~5000 ppm. The light sensor is BH1750, with a measurement range of 0-65535 lx.

For hardware implementation, the CC2538 chip is configured with a 32 MHz clock frequency to balance data processing speed and power consumption, and sensor nodes adopt an anti-interference shielding design to reduce signal attenuation in large venues with complex structures.

The network layer is mainly responsible for communication and data transmission. The system uses the Zigbee PRO protocol to construct a Mesh network topology, which includes three types of nodes: coordinator nodes, routing nodes, and terminal nodes. The coordinator node is deployed in the central control room of the venue, responsible for network initialization, address allocation, and data aggregation. Routing nodes are distributed throughout the venue to enhance signal coverage and achieve data relay. The terminal node (sensor node) is mainly responsible for data collection and transmission. The Mesh network topology of the venue is shown in Figure 2.

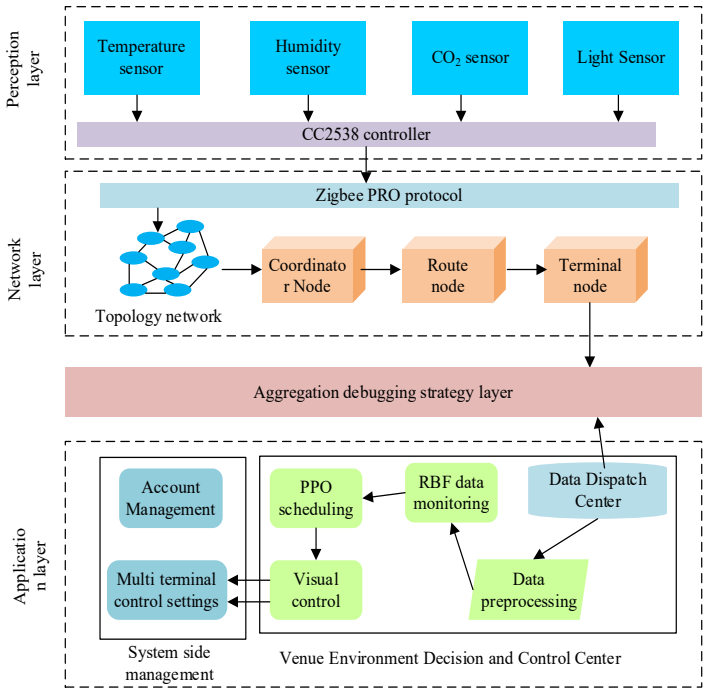

Figure 1: Framework diagram of venue environment regulation system

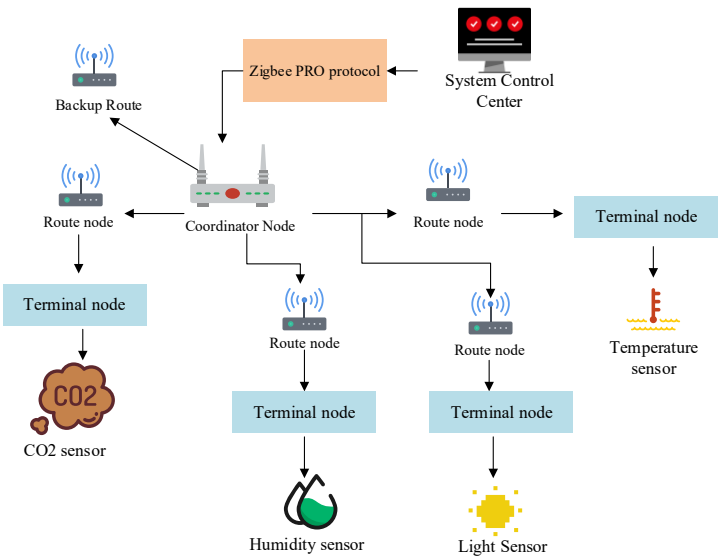

Figure 2: Venue mesh network topology structure

Figure 2 shows that a large number of terminal nodes are deployed in the venue to collect data from various sensors and transmit the data to the system data center through various routing nodes. In the application layer design, it communicates with the coordinator through Ethernet, supports real-time monitoring of multi-area parameters, historical data queries, and automatic dispatch of control

instructions. The application layer includes data storage, visualization, and decision control. It develops upper computer software using C# and MySQL to view and schedule environmental monitoring data. In addition, the system design takes into account the large number of terminal nodes deployed in the venue, which poses congestion and latency issues for data transmission. In response, the system network layer has set up a data aggregation strategy, which preprocesses the data of terminal nodes within its jurisdiction through routing nodes, and uses a weighted average algorithm to fuse multi-node data to alleviate communication pressure, as shown in equation (1) [13].

$$\bar{x} = \sum_{z=1}^{n} w_z x_z / \sum_{z=1}^{n} w_z \tag{1}$$

In equation (1), x_z is the measurement value of the z-th terminal node, w_z is the node adjustment weight, and n is the number of nodes in the region. The system introduces a low-power mechanism. The terminal nodes adopt periodic sleep mode, with a default sampling interval of 30 s. In addition, the routing nodes enable the "receive forward sleep" mode and turn off the RF module when idle. Through the above mechanism, the system power consumption has been optimized, and the requirements for venue environment regulation have been met.

2.2 Construction of Environmental Monitoring Model Based on Improved RBF

In the Zigbee-based venue environment control system, it already has the general ability to collect venue environment data. However, large venues have the characteristics of large spatial spans, severe fluctuations in pedestrian flow, and uneven heat dissipation of equipment, resulting in strong nonlinear and time-varying environmental parameters, making it difficult to accurately monitor scene data. This study proposes an improved RBF-based environmental parameter prediction model, which corrects real-time monitoring data and provides a decision-making basis for intelligent environmental regulation. The process of environmental parameter prediction technology based on improved RBF is shown in Figure 3.

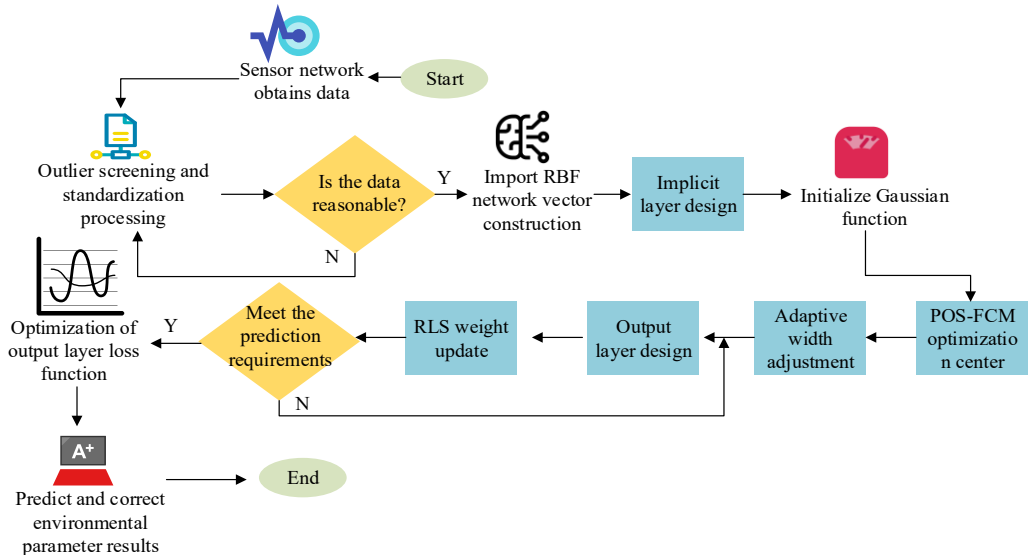

Figure 3: Process of environmental parameter prediction technology based on improved RBF

In Figure 3, the improved RBF adopts a three-layer structure of "input layer, hidden layer, output layer". Considering the shortcomings of traditional RBF models, such as center selection relying on experience and fixed-width parameters, this study introduces clustering algorithms and adaptive parameter methods to improve the model. In the improved RBF design, the input vector of its input layer is the historical environmental parameters collected by the Zigbee system, set as $X = [x_1, x_2, ..., x_n]$. x_i is the i-th monitoring parameter, such as x_1 for temperature and x_2 for humidity. n is the input dimension, selected based on the characteristics of the venue. The monitoring feature data before inputting RBF are used to remove sensor fault data using the 3σ criterion [14]. Meanwhile, normalization is introduced to map the data to the [0,1] interval, as shown in equation (2).

$$\hat{x} = \frac{x - x_{\min}}{x_{\max} - x_{\min}} \tag{}$$

In equation (2), $x_{\max}$ and $x_{\min}$ are the maximum and minimum values of the parameters. The RBF hidden layer is designed with m radial basis functions, and the output of the j-th neuron is shown in equation (3).

$$\phi_j(X) = \exp\left(-\frac{\| X - C_j \|^2}{2\sigma_j^2}\right) \tag{3}$$

In equation (3), $C_j = [c_{j1}, c_{j2}, ..., c_{jn}]$ is the center of the j-th basis function, σ_j is the width parameter, and $\|\cdot\|$ is the Euclidean distance. Considering the problem of model center selection, this study introduces clustering algorithms to optimize center selection [15]. Traditional K-means clustering is prone to getting stuck in local optima, so this study uses the Particle Swarm Optimization (PSO) algorithm to optimize Fuzzy C-Means (FCM) clustering as the optimization algorithm. The objective function is shown in equation (4).

$$J = \sum_{i=1}^{N}\sum_{j=1}^{m} u_{ij}^{q} \| X_i - C_j \|^2 \tag{4}$$

In equation (4), u_{ij} is the membership degree of sample x_i to cluster center C_j, q is the fuzzy coefficient, and N is the total number of samples. PSO iteratively optimizes u_{ij} and C_j to make the center more in line with the data distribution. In addition, this study introduces an adaptive width adjustment strategy to optimize the fixed width parameter problem of the RBF model. The width is set to σ_j. This study dynamically adjusts the sample density around the center C_j, as shown in equation (5) [16].

$$\sigma_j = k \cdot \frac{\max_{l \neq j} \| C_j - C_l \|}{\sqrt{2m}} \tag{5}$$

In equation (5), k is the density coefficient. C_l is the adjacent cluster center.

After improving RBF, the output layer adopts linear weighted summation to output the predicted value y, as shown in equation (6).

$$y = \sum_{j=1}^{m} w_j \phi_j(X) + b \tag{6}$$

In equation (6), w_j is the weight from the hidden layer to the output layer, and b is the bias term. In addition, setting the forgetting factor in RBF can affect the tracking ability of real-time data, so this study introduces the use of Recursive Least Squares (RLS) algorithm to correct the forgetting factor. The weight vector of the output layer at time k after correction is shown in equation (7).

$$\mathbf{w}(k) = \mathbf{w}(k-1) + \mathbf{K}(k)[d(k) - \phi(k)^T \mathbf{w}(k-1)] \tag{7}$$

In equation (7), $\mathbf{K}(k)$ is the gain matrix and $d(k)$ is the expected output. $\phi(k)$ is the output vector of the hidden layer at time k, which improves the tracking ability of time-varying data.

2.3 Modeling of Venue Environment Regulation Based on Deep Reinforcement Learning

By improving RBF, the system has achieved effective prediction of the dynamic parameters of the venue environment, thereby correcting environmental monitoring data. However, large venues have a large spatial span, and the parameters of each region face strong coupling problems. In addition, the monitoring parameters of the venue are highly dynamic, such as large fluctuations in crowd flow and parameter changes caused by equipment start and stop, which makes it difficult to meet the requirements of venue environmental scheduling. To address the aforementioned issues, this study proposes a Proximal Policy Optimization (PPO) algorithm based on improved reinforcement learning to construct a regulatory model. The PPO model framework is shown in Figure 4.

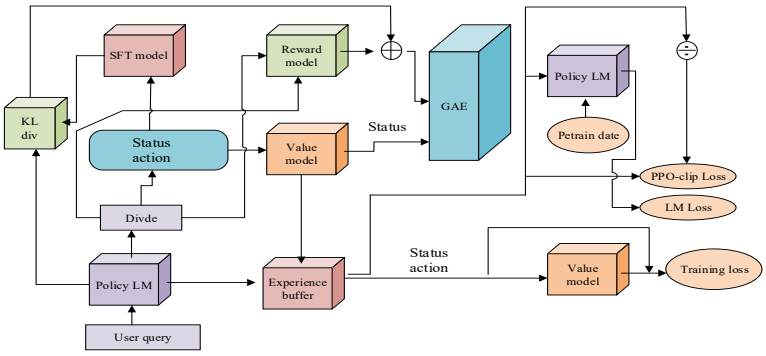

Figure 4: PPO model framework diagram

In Figure 4, the model adopts a "perception decision execution" closed-loop architecture, which includes three core requirements: state space, action space, and reward function design. The principle of environmental scheduling based on the PPO model is to collect real-time environmental parameters from the Zigbee sensor network and input them into the perception layer, combined with the short-term prediction results of the RBF model, to form state inputs. The decision-making layer uses PPO intelligent agents to output control actions based on the current state, such as air conditioning gear, fresh air volume, and other control parameters. Finally, the execution layer drives the device to perform actions through relay modules and infrared control modules, while feeding back the device's operating status to the perception layer, forming a closed-loop design. In state space design, the state needs to include real-time monitoring values and predicted values, reflecting the global characteristics S_t of the environment, as shown in equation (8).

$$S_t = \{T_t^1, ..., T_t^\beta, RH_t^1, ..., RH_t^\beta, C_t^1, ..., C_t^\beta, \hat{T}_{t+1}, RH_{t+1}, P_t\} \quad (8)$$

In equation (8), T_t^i, RH_t^i, and C_t^i represent the temperature, humidity, and CO_2 concentration of the i-th sensor at time t. β is the number of sensors. RH_{t+1} is the 1-hour mean predicted by the RBF model. P_t is the total power of the device. In venue environment monitoring, the Zigbee network status parameter update time is set to 10 seconds to ensure that the intelligent agent is aware of the environmental dynamics. In action space design, actions correspond to discrete operations of control devices, balancing control accuracy and device lifespan. The action space set A_t is shown in equation (9).

$$A_t = \{a_1, a_2, ..., a_n\} \quad (9)$$

In equation (9), a_k is the gear of the air conditioning/fresh air system (i.e. a_1 =off, a_2 =low speed,..., a_5 =high speed). n is the total number of gears, which is set according to the gear regulation of the devices in the environment. In addition, action constraints have been set to avoid frequent device switching, i.e. the gear difference between adjacent times is ≤ 2. In addition, in venue environment regulation, venue regulation needs to meet the requirements of energy consumption, regulation accuracy, and uniformity of regulation parameters. In response to this, a reward function R_t design that fully considers energy consumption FP, accuracy T_{sc}, and uniformity T_{unif} was introduced in the reward function design, as shown in equation (10) [17].

$$R_t = \alpha_1 T_{sc} + \alpha_2 T_{unif} + \alpha_3 FP \quad (10)$$

In equation (10), α_1, α_2, and α_3 are weight parameters corresponding to comfort, balance, and energy consumption. The expression of precision T_{sc} is shown in equation (11).

$$T_{sc} = -\sum_{i=1}^{\beta} |T_t^i - T_{set}| \quad (11)$$

In equation (11), T_{set} represents the environmental parameters set for the device, and T_t^i represents the current environmental parameters. The larger the T_{sc}, the higher the reward. The uniformity T_{unif} ensures the consistency of parameters in each region, and its calculation is shown in equation (12).

$$T_{unif} = -(\max(T_t^i) - \min(T_t^i)) \quad (12)$$

In equation (12), $\max(T_t^i)$ and $\min(T_t^i)$ are the maximum and minimum environmental parameters of the device. The smaller the temperature difference and the larger the T_{unif} in the region parameters, the more rewards will be obtained. The calculation of energy consumption FP is shown in equation (13).

$$FP = -\gamma \cdot P_t \quad (13)$$

In equation (13), γ is the energy consumption coefficient. In addition, venues are prone to uneven pedestrian flow, such as some areas being fully booked while others are not, resulting in significant differences in environmental regulation [18]. Therefore, in response to the high-dimensional state and multi-objective optimization requirements of the venue environment, two improvements have been made to the traditional PPO. Improvements include introducing spatial attention mechanisms, strengthening attention to densely populated areas, optimizing the objective function, and enhancing the accuracy of environmental regulation. This study adds an attention layer to the Actor network to focus the agent on key areas, as shown in equation (14) [19].

$$\mathrm{Att}(s_t^i) = \frac{\exp(s_t^i \cdot w)}{\sum_{j=1}^{\beta} \exp(s_t^j \cdot w)} \quad (14)$$

In equation (14), s_t^i is the state feature of the i-th sensor, w is the attention weight, and $\text{Att}(s_t^i)$ is the attention weight of the region. Additionally, traditional PPO editing strategies may overlook the trade-off of multi-objective rewards.

The expression of introducing the adaptive editing coefficient ε_t is shown in equation (15) [20].

$$\varepsilon_t = \max(0.1, 0.2 - 0.001 \cdot t) \quad (15)$$

In equation (15), t is the number of training steps. ε_t decays from 0.2 to 0.1 as the training progresses, balancing exploration and utilization. Finally, based on the adaptive editing coefficient ε_t, the Improved PPO (I-PPO) final objective function $L(\theta)$ can be obtained, as shown in equation (16).

$$L(\theta) = \mathrm{E}_t\left[\min\left(r_t(\theta)A_t, \text{clip}(r_t(\theta), 1-\varepsilon_t, 1+\varepsilon_t)A_t\right)\right] \quad (16)$$

In equation (16), $r_t(\theta)$ is the strategy ratio, and E_t represents the expectation at time t. A_t is the advantage function, which is the difference between the action value and the state value.

The entire process of venue environment control technology based on I-PPO is shown in Figure 5.

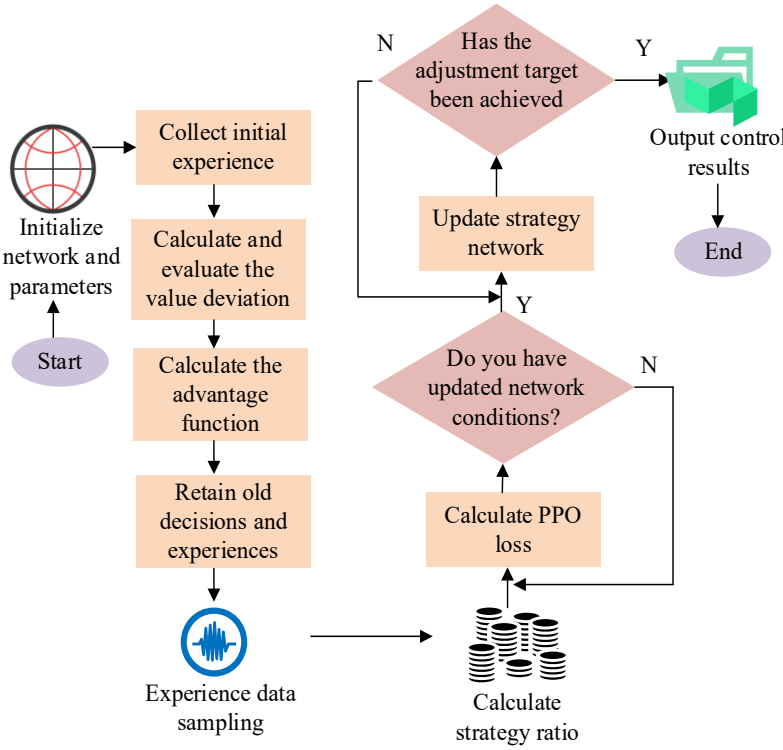

Figure 5: Venue environment control process based on I-PPO

This technology includes data preparation, network parameter initialization, interactive sampling, and policy updates. It updates and adjusts the dynamic targets (energy consumption, accuracy, uniformity) of the venue by improving PPO, ensuring a comfortable and fresh environmental experience in various areas of the venue.

3. Results and Analysis

3.1 Analysis of The Monitoring Effect of Venue Environment

To verify the effectiveness of the proposed technology in venue scene monitoring, it is compared with existing mainstream models. The experimental parameters are shown in Table 1.

In Table 1, this study conducted experimental analysis using a Windows 10 system, and venue monitoring services were provided using an Ubuntu 20.04 system. The experiment introduced professional datasets and self-made data for testing. The professional dataset was based on the ASHRAE Building Energy DataSets (ASHRAE), a publicly available dataset from the American Society of Heating, Refrigerating, and Air Conditioning Engineers. It contained data on humidity, temperature, wind speed, and a total of 53.6 million measurement records. To meet the requirements of venue environmental monitoring, this study collected data from a large sports venue to create a venue dataset. The venue had 3,000 audience seats and a building size of 15,000 m².

This study collected various scene data from July to October 2023, recording over 500 sensor monitoring data in the venue, totaling 150,000 valid data points, covering light intensity, CO_2 concentration, temperature, and light intensity. In the monitoring phase, this study compared the Long Short-Term Memory-Gated Recurrent Unit (LSTM-GRU) with Particle Swarm Optimization-Random Forest (PSO-RF) and improved RBF. For the improved RBF model, hyperparameter tuning was performed using a 5-fold cross-validation approach. The number of hidden layer neurons was searched in the range [15, 35] and optimized to 25. The fuzzy coefficient m of PSO-FCM was fixed at 2.0 after comparing values of 1.5, 2.0, and 2.5. The density coefficient λ in the adaptive width strategy was set to 0.8. The forgetting factor in the RLS algorithm was adjusted to 0.95 to balance real-time tracking and stability. Under a self-made dataset, the monitoring effects of different techniques on environmental humidity and temperature within 400 minutes were compared, as shown in Figure 6.

Table 1. Experimental environment

Project	Parameter
Experimental system	Windows 10
Development environment	Python 3.8
Data analysis	MATLAB 2022a
Processor	I7 9700K
Graphics card	RTX3070
Ram (random access memory)	32G
Hard disk	2t
Server	Ubuntu 20.04

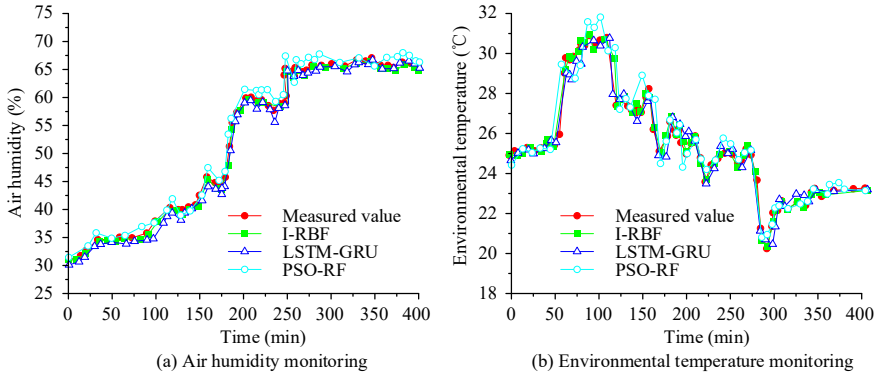

(a) Air humidity monitoring (b) Environmental temperature monitoring

Figure 6: Monitoring results of relative humidity and temperature in the environment

Figure 6 (a) shows the environmental humidity monitoring data, and the curve shows an increasing and gradually stable trend. The red curve represents the actual monitoring value, and the improved RBF model is closest to the actual monitoring curve with a monitoring accuracy of 97.25%. The second-best performance is LSTM-GRU, which has deviations from actual values in some periods, with a monitoring accuracy of 90.25%. PSO-RF has significant deviations from actual values in multiple time periods, with a final monitoring accuracy of 86.25%. Figure 6 (b) shows the results of environmental temperature monitoring. The environmental temperature shows a trend of first increasing, then gradually decreasing, and stabilizing at 22 ℃. The initial increase in foot traffic and rising weather temperatures causes the venue temperature to reach a maximum of 32 ℃, but as temperature regulation increases, the temperature gradually decreases to a stable level. The improved RBF is basically consistent with the actual monitoring values, and the overall monitoring accuracy is the best. The improved RBF, LSTM-GRU, and PSO-RF have final monitoring accuracies of 98.25%, 91.25%, and 84.86%. Based on a self-made dataset, monitoring errors are compared in different scene environments, as shown in Figure 7.

Figure 7 (a) shows 10 sets of humidity sensor monitoring data from different locations. The error of PSO-RF is the largest, with a maximum relative error of 5.01% in sensor 8. The maximum monitoring relative errors of LSTM-GRU and improved RBF are -2.12% and 1.02%. In Figure 7 (b), the improved RBF has the lowest monitoring error, with a maximum relative error of 0.87%, which is better than the 3.12% and -3.24% of LSTM-GRU and PSO-RF. Figure 7 (c) shows the monitoring of CO2 concentration. Similarly, both LSTM-GRU and PSO-RF show significant fluctuations, while the improved RBF has the smallest fluctuations and the error is controlled within the range of 1.22%, performing the best. In the illumination monitoring of Figure 7 (d), PSO-RF shows significant errors in multiple sets of sensor monitoring, with a maximum error of 38.72%. The maximum errors of LSTM-GRU and improved RBF are 37.8% and 1.32%. The improved RBF provides more accurate and effective monitoring of venue environmental data. In addition, a self-made dataset is selected to test the prediction time of different humidity sensor data, as shown in Figure 8.

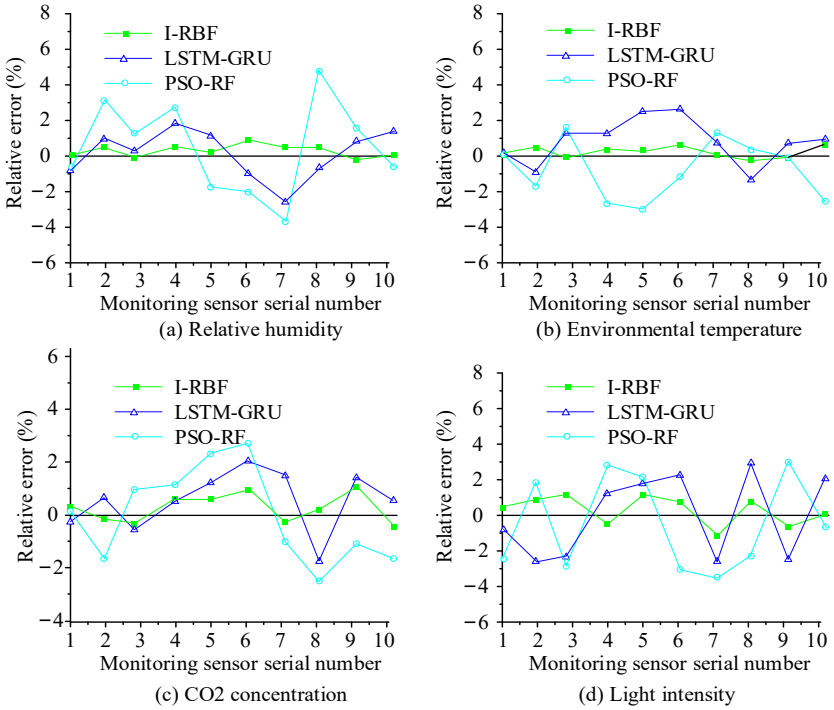

Figure 7: Relative error values of prediction in different scenarios

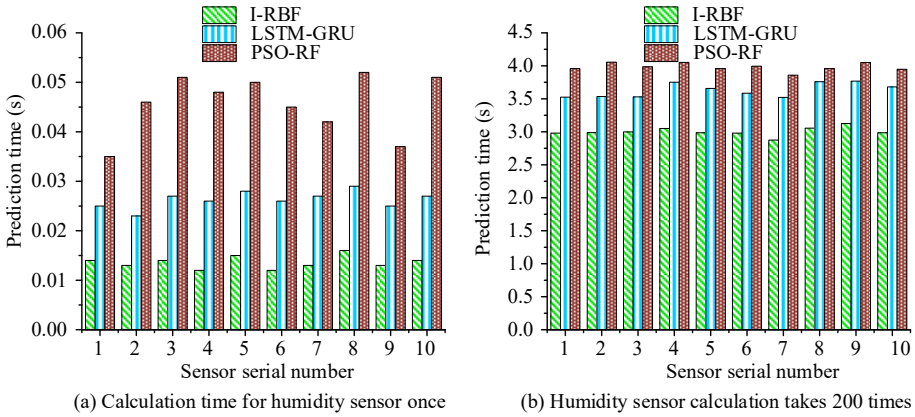

Figure 8: Comparison of prediction time consumption under different sensors

Figure 8 (a) shows the predicted time taken by the environmental humidity sensor to record once. Compared with other models, PSO-RF has the longest and most obvious fluctuation time for predicting environmental humidity data, with an average prediction time of 0.0452 s. LSTM-GRU and the improved RBF have shorter overall prediction time, with an average prediction time of 0.0251 s and 0.0286 s for environmental humidity. Figure 8 (b) shows the prediction time recorded 200 times.

The overall prediction time of PSO-RF is significantly higher than that of other models, with a maximum prediction time of 4.25 s for a single sensor, while PSO-RF and the improved RBF are 3.785 s and 3.215 s. The improved RBF model has excellent data processing performance and performs better.

3.2 Analysis of the Effect of Venue Environment Regulation

The venue environmental monitoring system has adopted an improved RBF to correct the environmental monitoring data. This study adopts an I-PPO model for venue environment regulation. Among them, the learning rate of the model is 0.0005, the discount factor is 0.98, and the strategy is updated every 2,048 experiences. The I-PPO model's hyperparameters are optimized via grid search combined with empirical verification: the learning rate is selected as 0.0005 after testing 0.0001, 0.0005, and 0.001. The discount factor is set to 0.98 (compared with 0.95 and 0.99). The batch size for policy updates is determined as 2048 (tested ranges [1024, 4096]). The initial adaptive clipping coefficient ε is 0.2 with a linear decay rate of 0.0001

per training step. The Actor-Critic network adopts 2 hidden layers with 128 neurons (verified against 64 and 256 neurons) to balance training efficiency and regulation precision.In addition, this study introduces Deep Deterministic Policy Gradient (DDPG) and Deep Q-Network (DQN) as comparative models. The comparison of temperature and humidity control effects in the venue is shown in Figure 9.

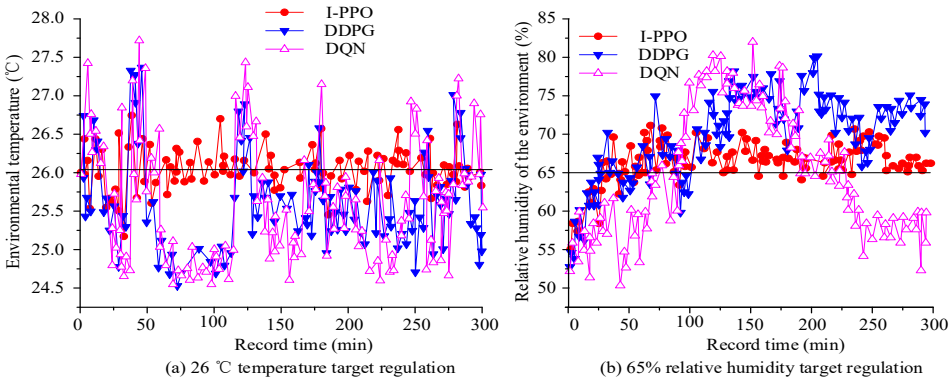

Figure 9: Comparison of target temperature regulation and relative humidity target regulation

In Figure 9 (a), the venue content has set a target temperature of 26 ℃, and the temperature control of the I-PPO model is closest to the target value, with a maximum temperature deviation of 0.71 ℃. Both DDPG and DQN have significant deviations, with maximum deviations of 1.565 ℃ and 1.782 ℃, indicating that the I-PPO achieves more accurate regulation. In Figure 9 (b), the target environmental humidity value is 65%, and the initial relative humidity of the environment is 55%. After regulation, the humidity of all three models has increased to the range of 65%. The curve regulation shows that DDPG has an over-regulation problem, that is, it continues to increase the regulation value after reaching the target value. DQN also has over-regulation issues, and there are abnormal regulations in the later stages, causing the humidity value to gradually decrease. Overall, the I-PPO regulation is the best, with a deviation controlled at 6.512% after stable regulation, showing the best overall performance.

The experiment selects the ASHRAE dataset to test the reward values of different models and the Root Mean Square Error (RMSE) values of temperature regulation, as shown in Figure 10.

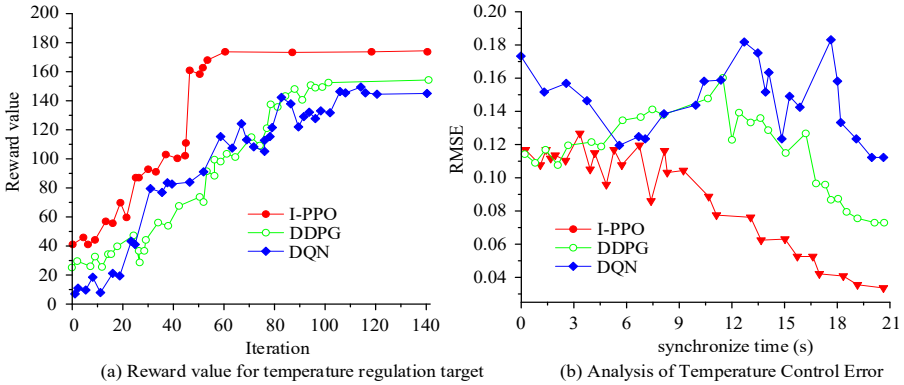

Figure 10: Comparison of reward value and temperature control error in professional dataset

In Figure 10 (a), the I-PPO model can converge the fastest and achieve the highest reward value of 180, which is better than the 156 and 146 of DDPG and DQN, indicating that the I-PPO target regulation is better. In Figure 10 (b), within a synchronization time of 21 seconds, the I-PPO model can optimize temperature regulation in the shortest possible time, resulting in a minimum RMSE of 0.001.

DDPG and DQN show significant fluctuations in the synchronous time regulation range, with the lowest RMSE of 0.118 and 0.072 for both. I-PPO has superior regulatory performance. Finally, based on the self-made dataset, the multi-objective regulation effects of different models are compared, as shown in Table 2.

Table 2. Multi objective regulation results of different models

Scene	Indicator	I-PPO	DDPG	DQN
Temperature control	Accuracy	0.975	0.912	0.858
	Uniformity (°C)	2.156	3.525	3.835
	Energy consumption (kW)	3.256	4.545	5.868
	System latency (s)	0.456	1.256	2.586
Relative humidity	Accuracy	0.956	0.895	0.826
	Uniformity (°C)	4.325	5.868	6.285
	Energy consumption (kW)	2.865	3.155	5.388
	System latency (s)	0.525	1.856	2.854
CO2 concentration	Accuracy	0.965	0.905	0.856
	Uniformity (°C)	80.25	101.566	156.685
	Energy consumption (kW)	1.556	2.385	2.885
	System latency (s)	0.624	2.546	3.584
Light intensity	Accuracy	0.975	0.902	0.859
	Uniformity (°C)	35.568	42.654	45.685
	Energy consumption (kW)	0.858	1.586	2.589
	System latency (s)	0.525	1.256	2.856

Table 2 shows that the regulation is tested based on a single device. In different environmental regulation scenarios, I-PPO performs the best in accuracy, uniformity, and energy consumption indicators. For example, in the light intensity test, the accuracy of I-PPO is 0.975, while DDPG and DQN are 0.902 and 0.859. In the same light uniformity test, the uniformity of I-PPO is 35.568 lx, lower than the 42.654 lx and 45.685 lx of DDPG and DQN. This indicates that I-PPO has more precise light regulation, and the overall performance is the best.

4. Summary

Large venues with high foot traffic and wide areas pose significant challenges to monitoring and regulating the environment inside the venues. In response to this, this study designed a venue environment control system based on Zigbee and Mesh, and optimized communication scheduling. To accurately monitor venue environmental data, this study used an improved RBF to construct an environmental parameter prediction model and achieve the correction of monitoring data. Finally, this study introduced the I-PPO model to construct a venue environment regulation model and introduced a spatial attention mechanism to optimize the regulation of densely populated areas. In environmental humidity monitoring, the improved RBF had a monitoring accuracy of 97.25%, which was better than the 90.25% of LSTM-GRU and 86.25% of PSO-RF. In multi-scenario monitoring errors, the maximum relative monitoring error of the improved RBF was 0.87%, which was lower than the 3.12% and -3.24% of LSTM-GRU and PSO-RF. In the temperature target regulation of the venue, the maximum temperature deviation of I-PPO was 0.71 ℃, which was better than the 1.565 ℃ and 1.782 ℃ of DDPG and DQN. In the comparison of temperature control errors in the ASHRAE dataset, I-PPO converged the fastest with a minimum RMSE of 0.001, which was lower than the 0.118 and 0.072 of DDPG and DQN. Overall, the proposed technology had good application effects. However, there are also shortcomings in this study, such as the fact that environmental scheduling is mainly based on conventional meteorological data and does not consider the impact of extreme and variable weather. In the future, multi-dimensional meteorological data can be integrated into system design, and data encryption can be strengthened to improve system stability and security.

References

[1] Inthasuth T, Kaewjumras Y, Sahapong Somwong W B. Comparative analysis of ZigBee, LoRa, and NB-IoT in a smart building: advantages, limitations, and integration possibilities. Int J Reconfigurable & Embedded Syst, 2025, 14(1): 165-175. DOI: 10.11591/ijres.v14.i1.

[2] Teng M, Al-Hamdawee Z M A, Ali A B M, Jin K, Ahmadi M. Integrating digital twins and neural networks for real-time temperature management in smart homes: An innovative approach using ZigBee networks. Energy Reports, 2025, 13(5): 6201-6218. DOI: 10.1016/j.egyr.2025.05.055.

[3] Cao S, Liu X, Li N. Environmental Protection Control System Based on IoT and Deep Learning Intelligent Monitoring Sensors. Scalable Computing: Practice and Experience, 2024, 25(4): 2210-2219. DOI: 10.12694/scpe.v25i4.2820.

[4] Jogekar A, Sinha P. Development of a wireless communication system for tracking environmental conditions from different locations of subterranean mines to the surface utilizing IoT based ZigBee modules. World Journal of Advanced Engineering Technology and

Sciences, 2025, 15(2): 2288-2299. DOI: 10.30574/wjaets.2025.15.2.0758.

[5] Ruzibaeva N, Makhmaraimova S, Khaydarov I, Mukhitdinova B. Application of Wireless Sensors in the Design of Smart Learning of the English Language Utilizing Zigbee Network Technology. J. Wirel. Mob. Networks Ubiquitous Comput. Dependable Appl., 2024, 15(3): 125-135. DOI: 10.58346/JOWUA. 2024. I3.009.

[6] Romputtal A, Phongcharoenpanich C. T-slot antennas-embedded ZigBee wireless sensor network system for IoT-enabled monitoring and control systems. IEEE Internet of Things Journal, 2023, 10(23): 20834-20845. DOI: 10.1109/JIOT.2023.3284005.

[7] Manikandan R, Ranganathan G, Bindhu V. Deep learning based IoT module for smart farming in different environmental conditions. Wireless Personal Communications, 2023, 128(3): 1715-1732. DOI: 10.1007/s11277-022-10016-5.

[8] Zhou Y, Cui X, Zhang Y. Self-powered wireless devices and machine learning enable local humidity monitoring. IEEE Transactions on Intelligent Transportation Systems, 2024, 25(8): 10369-10374. DOI: 10.1109/TITS.2024.3355384.

[9] Guo D, Luo D, Zhang Y, Zhnag X Y, Lai Y Y, Sun Y. Application of deep reinforcement learning to intelligent distributed humidity control system. Applied Intelligence, 2023, 53(13): 16724-16746. DOI: 10.1007/s10489-022-04320-7.

[10] Özen F, Kabaoğlu R O, Mumcu T V. Deep learning-based temperature and humidity prediction. Necmettin Erbakan Üniversitesi Fen ve Mühendislik Bilimleri Dergisi, 2023, 5(2): 219-229. DOI: 10.47112/neufmbd.2023.20.

[11] Kowalska A, Ashraf H. Advances in deep learning algorithms for agricultural monitoring and management. Applied Research in Artificial Intelligence and Cloud Computing, 2023, 6(1): 68-88. DOI: https://orcid.org/0000-0002-2419-4626.

[12] Li J, Fang Z, Wei D, Yan L. Flexible pressure, humidity, and temperature sensors for human health monitoring. Advanced healthcare materials, 2024, 13(31): 2401532. DOI: 10.1002/adhm.202401532.

[13] Wang L, Chen Z, Zou H, Huang D. A deep learning-based high-temperature overtime working alert system for smart cities with multi-sensor data. Nondestructive Testing and Evaluation, 2024, 39(1): 164-184. DOI: 10.1080/10589759.2023.2274008.

[14] Rahu M A, Shaikh M M, Karim S. IoT and machine learning solutions for monitoring agricultural water quality: a robust framework. Mehran University Research Journal of Engineering & Technology, 2024, 43(1): 192-205. DOI: 10.22581/muet1982.2401.2806.

[15] Bukhari S A S, Shafi I, Ahmad J. Enhancing flood monitoring and prevention using machine learning and IoT integration. Natural Hazards, 2025, 121(4): 4837-4864. DOI: 10.1007/s11069-024-06986-3.

[16] Raman R K, Kumar A, Sarkar S, Yadav A K, Mukherjee A. Reconnoitering precision agriculture and resource management: a comprehensive review from an extension standpoint on artificial intelligence and machine learning. Indian Research Journal of Extension Education, 2024, 24(1): 108-123. DOI: 10.54986/irjee/2024/jan_mar/108-123.

[17] Sudhakar M, Priya R M S. Computer vision-based machine learning and deep learning approaches for identification of nutrient deficiency in crops: A survey. Nature Environment and Pollution Technology, 2023, 22(3): 1387-1399. DOI: 10.46488/NEPT.2023.v22i03.025.

[18] Bilal A, Liu X, Long H, et al. Increasing crop quality and yield with a machine learning-based crop monitoring system. Comput Mater Continua, 2023, 76(2): 2401-2426. DOI: 10.32604/cmc.2023.0378.

[19] Mohseni S R, Zeitouni M J, Parvaresh A, et al. FMI real-time co-simulation-based machine deep learning control of HVAC systems in smart buildings: Digital-twins technology. Transactions of the Institute of Measurement and Control, 2023, 45(4): 661-673. DOI: 10.1177/01423312221119.

[20] Hebbi C, Mamatha H. Comprehensive Dataset Building and Recognition of Isolated Handwritten Kannada Characters Using Machine Learning Models. Artificial Intelligence and Applications, 2023, 1(3):179-190. DOI: 10.47852/bonviewAIA3202624.